Melt Transesterification of Bisphenol Acetophenone–Polycarbonate: A Kinetic Study

C. Godinez, L. J. Lozano

Department of Chemical and Environmental Engineering, Polytechnic University of Cartagena, 30202 Cartagena (Murcia), Spain

Received 30 May 2006; accepted 14 September 2006
DOI 10.1002/app.25507
Published online in Wiley InterScience (www.interscience.wiley.com).

ABSTRACT: This article deals with the development of kinetic parameters for bisphenol acetophenone–polycarbonate made by melt transesterification with diphenyl carbonate. The understanding of the influence of borosilicate glass of the reactor construction materials on the accuracy of the kinetic data is reported. During the development of analytical methods, the use of high performance liquid chromatography-mass spectrometry (HPLC-MS) was proven to be a valid tool to determine the oligomers existing in the reaction mixture. Accurate kinetics parameters were obtained by elimination of the interference of the construction materials. We provide the rate expressions, kinetic parameters [forward reaction frequency factor = $2.456 \times 10^{13} \pm 0.01$ $(cm^3/mol)^2/min$, forward reaction activation energy = 45.69 ± 0.2 kJ/mol, reverse reaction frequency factor = $2.068 \times 10^{14} \pm 0.01$ $(cm^3/mol)^2/min$, and reverse reaction activation energy = 56.37 ± 0.1 kJ/mol], and equilibrium constants at various temperatures. © 2006 Wiley Periodicals, Inc. J Appl Polym Sci 103: 4072–4079, 2007

Key words: activation energy; kinetics (polym.); modeling; polycondensation; step-growth polymerization

INTRODUCTION

The polycarbonate (PC) homopolymer based in bisphenol A (BPA) is commonly used in optical quality disk applications as the data matrix due to its favorable mechanical and optical properties. A lot of the current work has evolved around BPA PC, and therefore, its optical behavior is well understood.[1–6] To date, only two commercial production methods have been demonstrated to produce high quality PCs while remaining economically feasible. These processes are the two-phase interfacial process and the melt transesterification process. The transesterification method offers many advantages for the manufacture of PCs because the absence of solvents avoid solubility issues and eliminates the need for solvent separation–recycling loops and the unreacted monomers are always at trace levels (<1000 ppm) so that they can be easily degassed in the extruder, which enables direct pelletization right after the reaction.

However, fundamental studies of step copolymerization in the open literature are far less numerous than those on chain copolymerization. Although a lot of work has been done on the synthesis side of the problem, little quantitative kinetic data of copolycondensation has been reported (Mackey et al.,[7] Lopez-Serrano et al.,[8] Han,[9] Kim et al.,[10] and Lyoo et al.[11]). On top of that, some of the limitations of these earlier kinetic works laid in the accuracy of the experimental methods available, especially regarding the careful definition and control of the reaction conditions (e.g., monomer purity, catalyst addition and sampling, influence of construction materials on kinetics, temperature constraints by the boiling point of phenol, accurate reaction startup).

In this study, the transesterification of bisphenol acetophenone (BisAP) with diphenyl carbonate (DPC) was examined under a kinetic perspective, and the kinetic parameters for the BisAP–PC homopolymer were derived. These results were used as a previous step for determination of the kinetics of the BPA–BisAP–DPC system, which will be reported in a future article. BisAP was selected due to its chemical similarity with BPA and also because some authors[1,12,13] have claimed that it could reduce the intrinsic birefringence of BPA homopolycarbonate. In addition to the kinetic information, the values for the equilibrium constant were readily available. The equilibrium constant for this particular reaction was of primary importance because reversible polycondensation reactions can only achieve high conversions if the equilibrium is shifted byproduct removal. This information is a crucial parameter for the optimum design and operating conditions of further copolymerization processes.

Correspondence to: C. Godinez (carlos.godinez@upct.es).
Contract grant sponsor: Fundación Séneca, Government of the Region of Murcia; contract grant number: PPC/01445/03.

Journal of Applied Polymer Science, Vol. 103, 4072–4079 (2007)

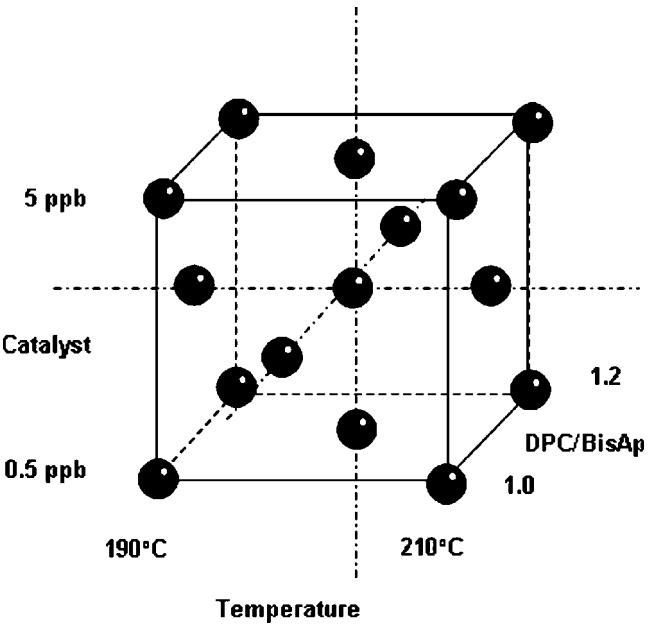

Figure 1 Factorial design of the experiments.

EXPERIMENTAL

Reagents

BisAP was 4,4′-(1-phenylethylidene) bisphenol (1571-75-1) was supplied by Aldrich Chemical Co. (Woodbury, NY), and DPC [102-09-0] was supplied by General Electric Co. (Cartagena, Spain). Both raw materials were greater than 99% in purity as claimed by the manufacturers, and they were used as supplied. Sodium hydroxide used as a catalyst and acetic acid used as a quencher were supplied by Panreac (Madrid, Spain).

Equipment and procedure

Batch melt transesterification experiments were conducted in a three-necked, round-bottom flask with a capacity of 250 mL. The reactor was kept in hydrochloric acid overnight and rinsed thoroughly with deionized water to minimize sodium contamination from the borosilicate reactors. The reactor was placed in a heating mantle with regulation capabilities. Temperature control was enabled by means of a J-type thermocouple located in the left neck of the reactor and a proportional-integral-differential (PID) controller. The reactor top was also heated and insulated so that condensation of phenol and low-molecular-weight oligomers could be prevented. The stirrer was placed in the central neck, and the right neck was used for catalyst introduction and sample extraction.

Two catalyst solutions (10^{-2} and 10^{-3} *M* NaOH) were prepared by the dissolution of solid NaOH in deionized water in a polypropylene volumetric flask. The reactor was charged with amounts of solid BisAP and DPC according to the experiment to be conducted (ca. 20–30 g each). The temperature was raised slowly to the desired temperature. Then, the catalyst solution was injected into the reactor with a microsyringe. This was considered the starting reaction time for all of the experiments.

The reactions were sampled at different times with disposable glass pipettes and immediately quenched in ice-water-cooled Erlenmeyer flasks and then dissolved in acetonitrile with 0.1% acetic acid in preparation for subsequent liquid chromatography analysis. Samples dissolved with only acetonitrile were found to reach their equilibrium composition in about 2 days due to the presence of residual sodium hydroxide catalyst. Therefore, samples had to be quenched with acetonitrile with a small amount of acetic acid.

A two-level composite factorial design was used for the settings of our experiments (Fig. 1). Temperature, catalyst, and initial DPC/BisAP molar ratio were chosen as experimental factors and yielded a total of 15 runs. Temperature levels (190–210°C) were constrained by the melting point of the monomeric mixture in the lower range and the boiling point of phenol in the upper range. Catalyst levels (0.5–5 ppm) were chosen on the basis of reactions rates observed to allow for reaction times that were slow enough to measure the data accurately. The initial DPC/BisAP molar ratio levels (1–1.2) were chosen to resemble those used in current manufacturing practices. For each run, 10 samples were withdrawn from the reactor, making a total of 150 times versus composition pairs of data, which were used for the kinetic analysis. Table I summarizes the experimental space.

Analytical method

The composition of the reaction mixture was determined by HPLC with a method described by Bailly et al.[14] and slightly adapted for our mixture. The

TABLE I
Composite Factorial Design of the Experiments

Experiment	Temperature (°C)	DPC/BisAP (molar ratio)	[Na] (ppb)
1	190	1.2	0.5
2	210	1.0	0.5
3	210	1.1	2.75
4	200	1.0	2.75
5	190	1.2	5.0
6	210	1.2	0.5
7	210	1.2	5.0
8	190	1.1	2.75
9	190	1.0	5.0
10	210	1.0	5.0
11	200	1.1	0.5
12	200	1.1	5.0
13	200	1.2	2.75
14	190	1.0	0.5
15	200	1.1	2.75

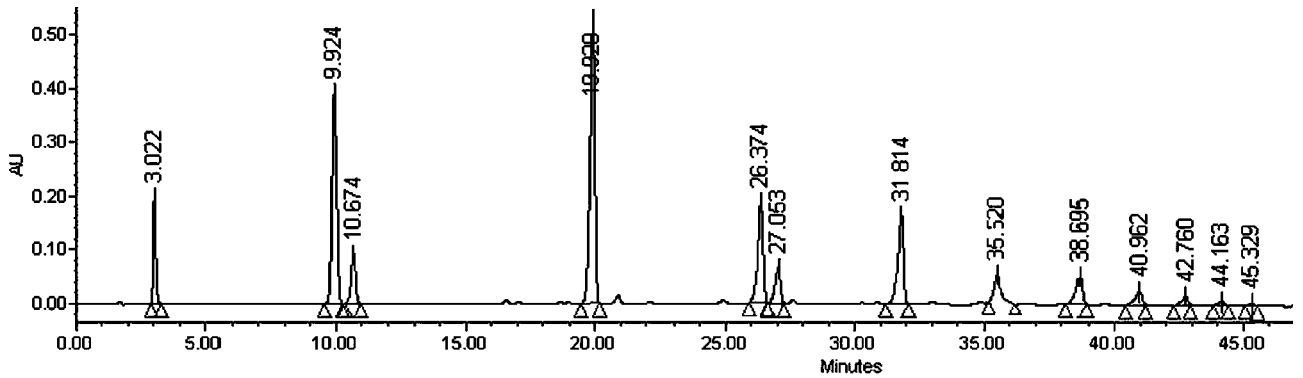

Figure 2 HPLC chromatogram under reaction conditions.

components were separated on a Waters X-Terra C18 column (Naters, Milford, MA) (i.d. = 150 × 2.1 mm) with 0.2% acetic acid (phase A) and acetonitrile (phase B) as the mobile phase. Gradient elution was as follows: 0 min and 40% B, 3 min and 40% B, 40 min and 100% B, and 45 min and 100% B at a flow of 1 mL/min. The detector used was a UV–visible diode array at a constant wavelength of 245 nm. A HPLC chromatogram for a sample under reaction conditions is presented in Figure 2.

The qualitative identification of phenol, BisAP, and DPC was performed by the injection of pure components alone (with peaks at 3, 10, and 11 min, respectively). However, this way of identification was impossible for the oligomers (with peaks at times higher than 19 min) because there were no commercial samples available and neither the concentration by preparative HPLC nor chemical synthesis were feasible for our group. Therefore, the qualitative identification of the oligomers was conducted with a mass spectrometer detector online with the UV–visible detector. This coupling allowed us to determine the fragmentation pattern of the molecules being eluted at a given time and, therefore, to compare those with the molecular masses of the oligomers, which were known from their molecular structure. According to Kim et al.'s[15] nomenclature, three kinds of oligomers were expected for the BisAP–DPC system: dihydroxyl endcapping oligomers (A_n's), diphenyl endcapping oligomers (B_n's), and monophenyl endcapping oligomers (C_n's), with n being the number of structural repeating units in the polymer chain. Their formulas are shown in Figure 3.

As pointed out by Bailly et al.[14] and Kim et al.[15] in a similar study for BPA PC, for species having the same number of phenyl carbonate groups (e.g., B_n, C_{n+1}, and A_{n+1}), the polar hydroxyl groups of C_{n+1} and A_{n+1} oligomers tend to increase retention time with respect to B_n oligomers. Also, A_{n+1} oligomers having bulkier bisphenol terminal groups elute after C_{n+1} oligomers. This observation, along with the HPLC-MS spectra, helped us to fully identify the sequence of oligomers (up to $n = 8$) that were present in our mixtures. An example for the DPC–BisAP–DPC trimer (weight-average molecular weight = 606 g/mol) mass spectrum is presented in Figure 4.

Kinetic model

Since early 1980s, several models to describe the BPA PC melt transesterification with DPC kinetics have been reported (Ravindranath and Mashelkar,[16] Hersh and Choi,[17] Kim et al.[15]). For modeling the polymerization kinetics, we used the molecular species model used by Kim et al.[15] This model tracks every component in the reaction mixture and the molecular weight of each macromolecule. There were only two functional end groups, and the only way for them to react (with side reactions that were negligible at low conversions ignored) was according to the following reactions:

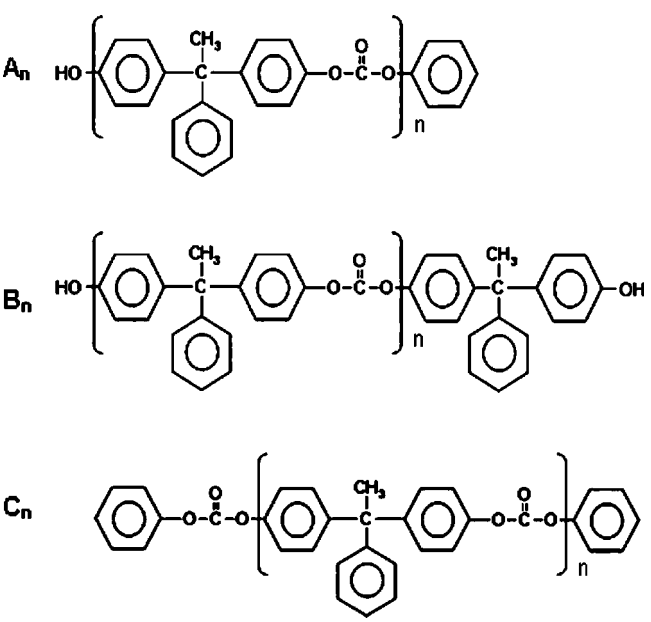

Figure 3 Molecular species used in the kinetic model.

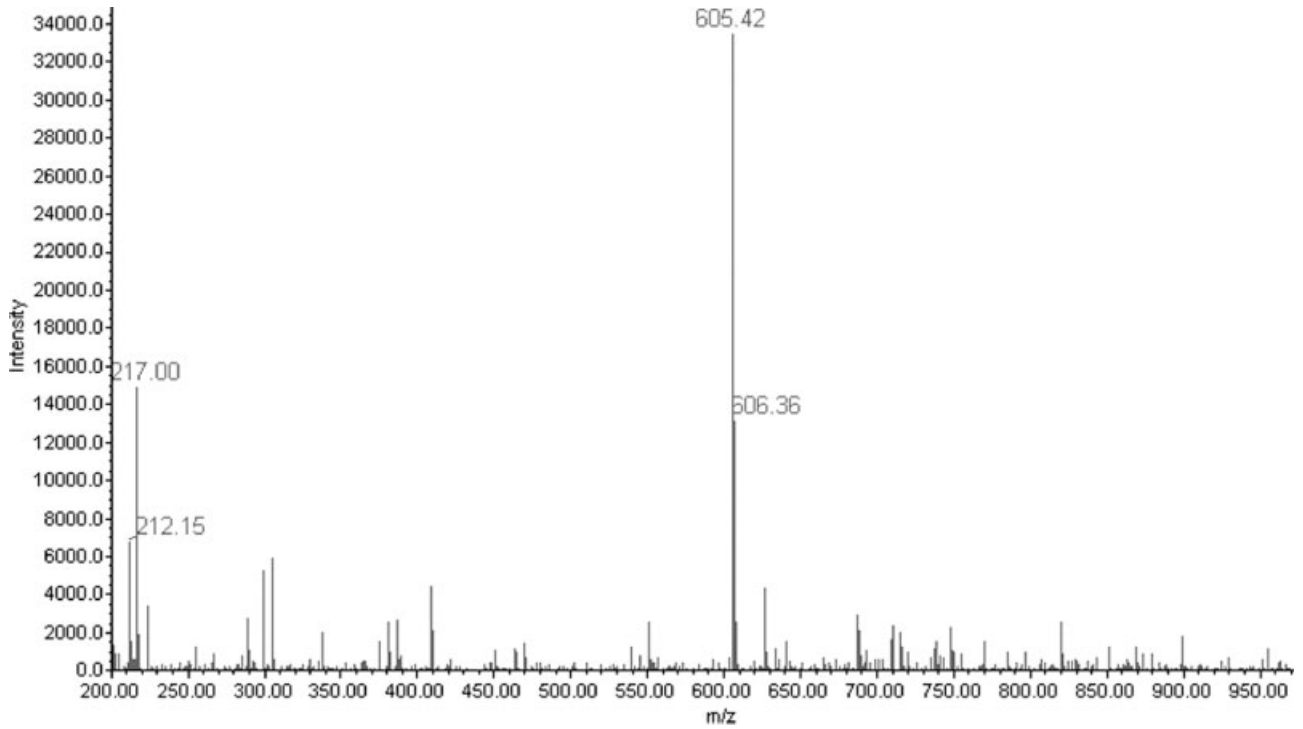

Figure 4 Mass spectrum of the DPC–BisAP–DPC trimer eluted by HPLC.

$$\mathrm{A}_n + \mathrm{B}_m \leftrightarrow \mathrm{C}_{n+m+1} + \mathrm{P}$$

$$\mathrm{A}_n + \mathrm{C}_m \leftrightarrow \mathrm{A}_{n+m} + \mathrm{P}$$

$$\mathrm{B}_n + \mathrm{C}_m \leftrightarrow \mathrm{C}_{n+m} + \mathrm{P}$$

$$\mathrm{C}_n + \mathrm{C}_m \leftrightarrow \mathrm{C}_{n+m} + \mathrm{P}$$

where m and n are the number of structural repeating units in the polymer chain and P is phenol.

With the assumption that the reactivities of the functional groups were independent of chain length, the component material balances could be derived for isothermal reaction conditions. Independent reactions were derived for the concentrations of BisAP (A_0), DPC (B_0), and phenol (P) and the concentrations of dihydroxyl endcapping oligomers (A_n), diphenyl endcapping oligomers (B_n), and monophenyl endcapping oligomers (C_n):

$$\frac{dA_0}{dt} = n_{\mathrm{cat}}\frac{1}{V^2}\left(-4k_fA_0B_0 - 4k_fA_0\sum_{m=1}^{\infty}B_m + k_rP\sum_{m=1}^{\infty}C_m - 2k_fA_0\sum_{m=1}^{\infty}C_m + 2k_rP\sum_{m=1}^{\infty}A_m\right) \quad (1)$$

$$\frac{dB_0}{dt} = n_{\mathrm{cat}}\frac{1}{V^2}\left(-4k_fA_0B_0 - 4k_fB_0\sum_{m=1}^{\infty}A_m + k_rP\sum_{m=1}^{\infty}C_m - 2k_fB_0\sum_{m=1}^{\infty}C_m + 2k_rP\sum_{m=1}^{\infty}B_m\right) \quad (2)$$

$$\frac{dC_1}{dt} = n_{\mathrm{cat}}\frac{1}{V^2}\left(4k_fA_0B_0 - k_rPC_1 - 2k_fC_1B_0. - 2k_fC_1\sum_{m=1}^{\infty}B_m - 2k_fC_1A_0 - 2k_fC_1\sum_{m=1}^{\infty}A_m + 2k_rP\sum_{m=1}^{\infty}A_m - 2k_fC_1\sum_{m=1}^{\infty}C_m + 2k_rP\sum_{m=2}^{\infty}C_m\right) \quad (3)$$

$$\frac{dP}{dt} = n_{\mathrm{cat}}\frac{1}{V^2}\left[4k_fA_0B_0 + 4k_fA_0\sum_{m=1}^{\infty}B_m + 4k_fB_0\sum_{m=1}^{\infty}A_m + 4k_f\sum_{m=1}^{\infty}A_m\sum_{j=1}^{\infty}B_j - k_rP\sum_{m=1}^{\infty}mC_m + 2k_fB_0\sum_{m=1}^{\infty}C_m + 2k_f\sum_{m=1}^{\infty}B_m\sum_{j=1}^{\infty}C_j - 2k_rP\sum_{m=1}^{\infty}mB_m + 2k_fA_0\sum_{m=1}^{\infty}C_m + 2k_f\sum_{m=1}^{\infty}A_m\sum_{j=1}^{\infty}C_j - 2k_rP\sum_{m=1}^{\infty}mA_m + k_f\sum_{m=1}^{\infty}C_m\sum_{j=1}^{\infty}C_j - k_rP\sum_{m=2}^{\infty}(m-1)C_m \quad (4)$$

$$\frac{dA_n}{dt} = n_{\mathrm{cat}}\frac{1}{V^2}\left(-4k_fA_nB_0 - 4k_fA_n\sum_{m=1}^{\infty}B_m + k_rP\sum_{m=n+1}^{\infty}C_m - 2k_fA_n\sum_{m=1}^{\infty}C_m + 2k_fA_0C_n + 2k_f\sum_{m=1}^{n-1}A_mC_{n-m} - 2k_{-1}PnA_n + 2k_{-1}P\sum_{m=n+1}^{\infty}A_m\right) \quad (5)$$

TABLE II
Repeatability Study for the Materials Used for the Construction of the Reactors

	Untreated borosilicate	HCl-treated borosilicate	Quartz
Repeatability (%)	41	21	8
Reproducibility (%)	9	10	8
Total GR&R[a] (%)	42	23	11

[a] GR&R, gage repeatability and reproducibility.

$$\frac{dB_n}{dt} = n_{cat}\frac{1}{V^2}\left(-4k_fB_nA_0 - 4k_fB_n\sum_{m=1}^{\infty}A_m + k_rP\sum_{m=n+1}^{\infty}C_m - 2k_fB_n\sum_{m=1}^{\infty}C_m + 2k_fB_0C_n + 2k_f\sum_{m=1}^{n-1}B_mC_{n-m} - 2k_rPnB_n + 2k_rP\sum_{m=n+1}^{\infty}B_m\right) \quad (6)$$

$$\frac{dC_n}{dt} = n_{cat}\frac{1}{V^2}\left[4k_f\sum_{m=0}^{n-1}A_mB_{n-m-1} - k_rPnC_n - 2k_fC_nB_0 - 2k_fC_n\sum_{m=1}^{\infty}B_m + 2k_rP\sum_{m=n}^{\infty}B_m - 2k_fC_nA_0 - 2k_fC_n\sum_{m=1}^{\infty}A_m + 2k_rP\sum_{m=n}^{\infty}A_m - 2k_fC_n\sum_{m=1}^{\infty}C_m + k_f\sum_{m=1}^{n-1}C_mC_{n-m} - k_rP(n-1)C_n + 2k_rP\sum_{m=n+1}^{\infty}C_m\right] \quad (7)$$

where k_f is the forward reaction kinetic constant and k_r is the reverse reaction kinetic constant. Because $n = 8$ in our case, we had a set of 13 differential equations describing the continuity of the system. The model equations were integrated by a fourth-order Runge–Kutta technique given initial conditions. A Marquardt algorithm was applied for the nonlinear regression of the data. In a second stage, the temperature dependence of the parameters was determined from an Arrhenius plot.

RESULTS AND DISCUSSION

One surprising finding was the tremendous influence of the reactor construction material on the accuracy of the kinetic data. To our knowledge, this has never been reported before. Traditionally, kinetic experiments have been performed on standard borosilicate glass reactors. We found that the repeatability and reproducibility (R&R) of the experiments were highly sensitive to this material, probably because the borosilicate glass contained significant amounts of active sodium, which is the catalyst of many polycondensation reactions.

We tested the effect by performing a statistical test comparing the conversion obtained under identical experimental conditions with that of the standard untreated borosilicate glass and with a pure quartz reactor. Also, a comparison was conducted with borosilicate glass submerged in 1*M* hydrochloric acid for 1 day and rinsed thoroughly with deionized water. The results of these comparisons are reported in Table II by the method described in the Appendix. As shown, repeatability was enhanced by both the treated borosilicate glass and the quartz. We finally conducted our experiments with HCl-treated borosilicate glass for economic reasons.

The evolution of BisAP as a function of time and temperature is presented in Figure 5 (with other variables equal at DPC/BisAP = 1.1 and [Na] = 2.75). It was remarkable that equilibrium was rapidly established in less than 30 min of reaction and that the agreement between the model predictions and the experimental data was quite reasonable. The same comparison is illustrated for the rest of the components in the reaction mixture for experiment 3 (190°C, DPC/BisAP = 1, [Na] = 5 ppb) as a function of time in Figure 6. Figure 6 illustrates the capability of the model for predicting the fine details of transesterification reactions. As shown, some of the oligomers did not seem to be in equilibrium, but all of the monomers, the phenol byproduct, and most of the oligomers were. Samples were taken additionally at 90 and 120 min after startup, but they are not shown in the graph for sake of clarity. On the other hand, 60 min was the residence time for the mixing drum in the commercial plant. Therefore, we used this time to represent the mixture composition after this vessel.

The forward and reverse transesterification rate constants were estimated from the differential rate data (including the whole concentration range but excluding those data under equilibrium to increase the accuracy of the results). Kinetic parameters (k_f and k_r) were obtained by residual sum of squares

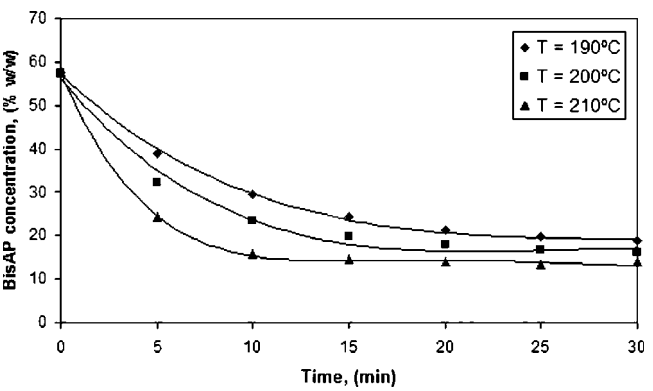

Figure 5 Effect of reaction temperature on the BisAP concentration profiles (DPC/BisAP = 1.1, [Na] = 2.75 ppb).

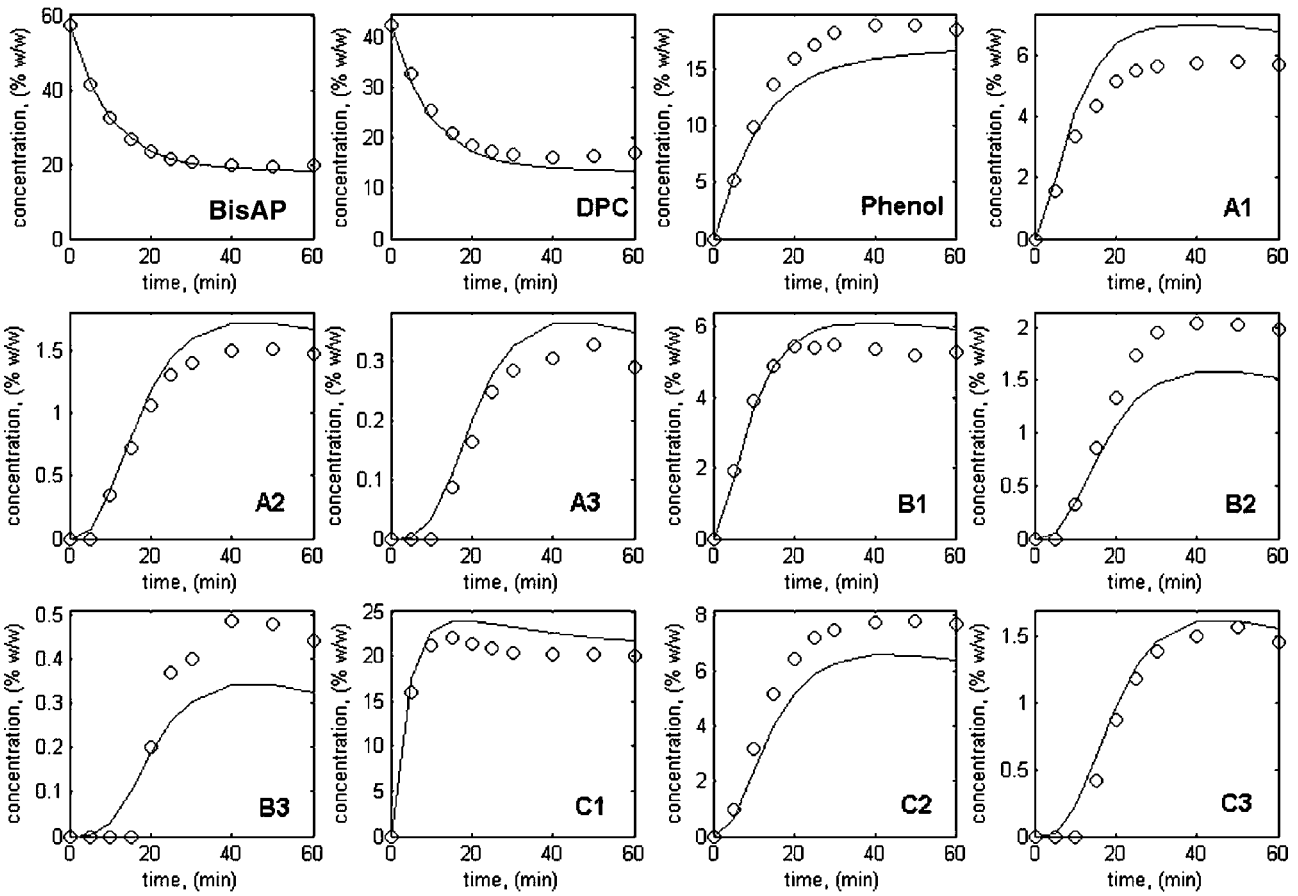

Figure 6 Evolution of the composition of the different reaction products as a function of time at 190°C, DPC/BisAP = 1.0, and [Na] = 5 ppb.

minimization with the Marquardt technique. As a result, the following parameters were obtained for k_f and k_r, respectively:

$$k_{0f} = 2.456 \times 10^{13} \pm 0.01 \text{ (cm}^3\text{/mol)}^2 \cdot \text{min}^{-1},$$
$$E_f = 45.69 \pm 0.2 \text{ kJ/mol}$$

$$k_{0r} = 2.068 \times 10^{14} \pm 0.01 \text{ (cm}^3\text{/mol)}^2 \cdot \text{min}^{-1},$$
$$E_r = 56.37 \pm 0.1 \text{ kJ/mol.}$$

where k_{0f} is the forward reaction frequency factor, E_f is the forward reaction activation energy, k_{0r} is the reverse reaction frequency factor, and E_r is the reverse reaction activation energy.

Figure 7 shows the Arrhenius plots for both kinetic constants in our experimental temperature range. These parameters were in the range of those obtained for BPA homopolycarbonate (Kim et al.[15]). The small difference in activation energies indicated that the apparent heat of reaction was small. From these data, an estimated value of the reaction enthalpy (ΔH_r) of −10.67 kJ/mol was derived. This value was in agreement with similar observations reported for other high-temperature transesterification processes (e.g., polyethylene terephthalate from Gupta and Kumar[18]).

The effect of catalyst concentration was also investigated, and the experimental results are shown in Figure 8 for the three catalyst concentrations at 200°C. As was expected, the effective kinetic constants were linearly dependent in the catalyst concentration range with a nonzero ordinate for [Na] = 0, which suggested that the effective rate constant (k') could be expressed as

$$k' = k_u + k_c[\text{Na}] \tag{8}$$

where k_u is the rate constant for the uncatalyzed reaction and k_c is the rate constant for the catalyzed reaction. In our case

$$k'_f = 0.0179 + 0.045[\text{Na}]$$

$$k'_r = 2.2064 + 4.9817[\text{Na}]$$

where k'_f is the effective forward reaction kinetic constant and k'_r is the effective reverse reaction kinetic constant.

Finally, from the values of the kinetic parameters, the equilibrium constants were derived as the ratio k_f/k_r. These values at 190, 200, and 210°C were 1.902, 1.754, and 1.696, respectively, showing a reverse constant that was more sensitive to temperature than the forward reaction, as expected from exothermic reactions.

CONCLUSIONS

In this article, we presented the kinetic parameters and equilibrium constant for catalyzed melt transesterification of BisAP and DPC. BisAP is an interesting monomer to be used as a comonomer in the manufacture of high-optical-quality resins. From the kinetic experiments conducted, a significant effect of the construction materials was observed, which was derived in an improved method for increasing the accuracy of kinetic data. Also, HPLC-MS was proven to be a valid technique for the traceability of the evolution of the oligomers during the reaction. A general model adapted for BisAP reaction was applied to derive the kinetic parameters. The parameters obtained were in a similar range to those reported for BPA, which enhanced the validity of our results. Also, from these data, an estimation of ΔH_r and the equilibrium constants was reported.

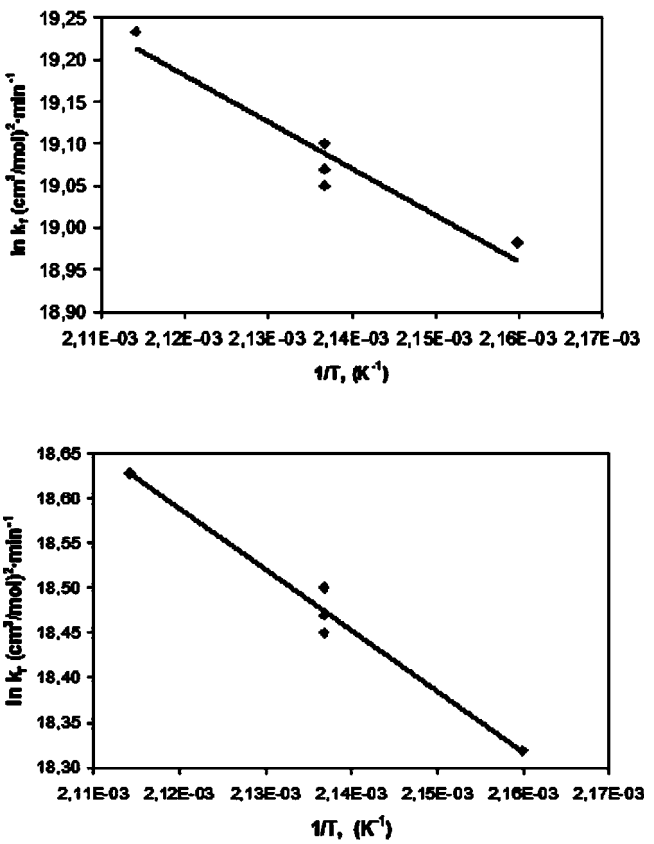

Figure 7 Arrhenius plots for k_f and k_r of the BisAP melt transesterification reaction.

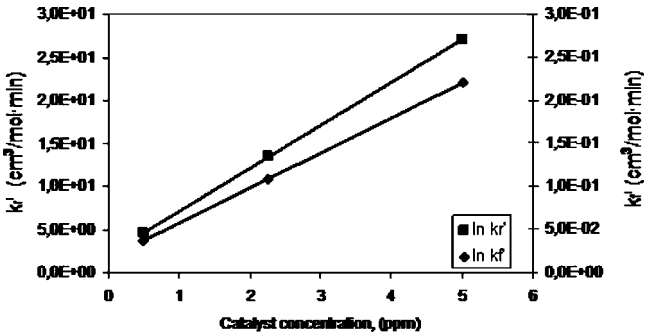

Figure 8 Effect of catalyst concentration on the normalized kinetic constants at 200°C.

NOMENCLATURE

α	Tabulated constant for the repeatability
A_0	Concentration of BisAP in the liquid phase (mol/cm^3)
A_n	Dihydroxyl endcapping oligomer
A_n	Concentration of dihydroxyl oligomers in the liquid phase (mol/cm^3)
β	Tabulated constant for the reproducibility
B_0	Concentration of DPC in the liquid phase, mol/cm^3
B_n	Diphenyl endcapping oligomer
B_n	Concentration of diphenyl endcapping oligomers in the liquid phase (mol/cm^3)
C_n	Monophenyl endcapping oligomer
C_n	Concentration of monophenyl endcapping oligomers in the liquid phase (mol/cm^3)
ΔH_r	Reaction enthalpy (kJ/mol)
E_f	Forward reaction activation energy (kJ/mol)
E_r	Reverse reaction activation energy (kJ/mol)
k'	Effective rate constant [(cm^3/mol)^2/min]
k_{0f}	Forward reaction frequency factor [(cm^3/mol)^2/min]
k_{0r}	Reverse reaction frequency factor [(cm^3/mol)^2/min]
k_c	Kinetic constant for the catalyzed reaction [(cm^3/mol)^2/min]
k_f	Forward reaction kinetic constant [(cm^3/mol)^2/min]
k_f'	Effective forward reaction kinetic constant [(cm^3/mol)^2/min]
k_r	Reverse reaction kinetic constant [(cm^3/mol)^2/min]
k_r'	Effective reverse reaction kinetic constant [(cm^3/mol)^2/min]
k_u	Kinetic constant for the uncatalyzed reaction [(cm^3/mol)^2/min]
n_{cat}	Moles of catalyst (mol)
P	Phenol
P	Concentration of phenol in the liquid phase (kmol/m^3)
$\overline{\overline{R}}$	Sum of the ranges for all of the series of data

T Tolerance
V Reactor volumen, cm^3
$\overline{X}_{diff}$ Difference between the maximum and minimum values of all of the averages

APPENDIX: R&R STUDIES

To guarantee the quality of any experimental data, we must be able to quantify the variability in the results introduced by the experimental setup itself (repeatability) and/or the variability due to the people that handle it (reproducibility).

To evaluate these metrics, one must perform a test in which several samples are measured three times (trials) by three different operators (Box et al.[19] and Juran and Godfrey[20]). For each sample and operator, one must calculate the average for all of the measurements and the difference between the higher and lower values obtained (ranges). With these data, R&R can be computed with

$$EV = \overline{\overline{R}}\,\alpha \tag{A.1}$$

$$AV = \sqrt{(\overline{X}_{diff}\beta) - \frac{\overline{\overline{R}}^2\alpha^2}{n \times m}} \tag{A.2}$$

$$R\ \&\ R = \frac{\sqrt{EV^2 + AV^2}}{T} \times 100 \tag{A.3}$$

where EV is the repeatability (equipment variability), AV is the reproducibility (appraiser variability), $\overline{\overline{R}}$ is the sum of the ranges for all of the series of data, $\overline{X}_{diff}$ is the difference between the maximum and minimum values of all of the averages of the series of data, and T is the so-called tolerance, or minimum accuracy required for the test. The constants for the repeatability (α) and reproducibility (β) were tabulated depending on the number of trials and number of operators used in the test.

According to eq. (A.3), R&R is defined as the ratio of the lumped EV and AV to the process T. Therefore, contrarily to what is intuitively understood, a low R&R means that the overall variability in our measurement system did not interfere with the process. Juran and Godfrey[20] indicated that a R&R higher than 30% is not acceptable as a measurement system due to its lack of repeatability. The dissection of the contributions gives an idea of whether we have a human problem (operators need more training) or a problem in the measurement system (we must investigate and solve the problem to reduce variability). A gage R&R between 10 and 30% is acceptable depending on the application and the T values. A gage R&R below 10% is a valid measurement system.

References

1. Philipp, H. R.; LeGrand, D. G.; Cole, H. S.; Liu, Y. S. Polym Eng Sci 1987, 27, 1148.
2. Emmelius, M.; Pawloski, G.; Vollmann, H. W. Angew Chem Int Ed Engl 1989, 28, 1445.
3. Henning, J. Jpn J Appl Phys 1987, 24(4; Suppl. 26), 9.
4. Erman, B.; Marvin, D. C.; Irvine, P. A.; Flory, P. J. Macromolecules 1982, 15, 664.
5. Floudas, G.; Lappas, A.; Fytas, G.; Meier, G. Macromolecules 1990, 23, 1747.
6. Riande, E.; Saiz, E. Dipole Moments and Birefringence of Polymers; Prentice Hall: Upper Saddle River, NJ, 1992.
7. Mackey, J. H.; Pattison, V. A.; Pawlak, J. A. J Polym Sci 1978, 16, 2849.
8. Lopez-Serrano, F.; Castro, J. M.; Macosko, C. W.; Tirrell, M. Polymer 1980, 21, 263.
9. Han, M. J. Macromolecules 1980, 13, 1009.
10. Kim, J. H.; Lee, S. Y.; Park, J. H.; Lyoo, W. S.; Noh, S. K. J Appl Polym Sci 2000, 77, 693.
11. Lyoo, W. S.; Lee, S. G.; Ha, W. S.; Lee, J.; Kim, J. H. Polym Test 2000, 19, 299.
12. Legrand, D. G.; Olszewski, W. V.; Bendler, J. T. Thermochim Acta 1990, 166, 105.
13. Legrand, D. G.; Olszewski, W. V.; Bendler, J. T. J Polym Sci Part B: Polym Phys 1987, 25, 1149.
14. Bailly, C.; Daoust, D.; Legras, R.; Mercier, J. P., de Valck, M. Polymer 1986, 27, 776.
15. Kim, Y.; Choi, K. Y.; Chamberlain, T. Ind Eng Chem Res 1992, 31, 2118.
16. Ravindranath, K.; Mashelkar, R. A. J Appl Polym Sci 1982, 27, 2625.
17. Hersh, S. N.; Choi, K. Y. J Appl Polym Sci 1990, 41, 1033.
18. Gupta, S.; Kumar, A. Reaction Engineering of Step Growth Polymerization; Plenum: New York, 1987.
19. Box, G. E. P.; Hunter, W. G.; Hunter, J. S. Statistics from Experimenters: An Introduction to Design, Data Analysis and Model Building; Wiley: New York, 1978.
20. Juran, J. M.; Godfrey, A. B. Juran's Quality Handbook; McGraw-Hill: New York, 2001.